# Spin Distributions, Ring Conformations, and Spiroconjugation in "Phosphaverdazyl" Radicals

**Robin G. Hicks,*[,1] Lars Öhrström,*[,2] and Greg W. Patenaude[1]**

Department of Chemistry, University of Victoria, P.O. Box 3065, Victoria, British Columbia V8W 3V6, Canada, and Institutionen för Oorganisk kemi, Chalmers Tekniska Högskola, SE-412 96, Göteborg, Sweden

*Received August 15, 2000*

Reaction of *P*-dimethylaminophosphonic acid bis(1-methylhydrazide) (**6**) with trimethyl orthobenzoate gave 1,2,5,6-tetrahydro-1,5-dimethyl-6-(*N*,*N*-dimethylamino)-6-phenyl-1,2,4,5,6-tetrazaphosphorine-6-oxide (**7**), which was subsequently oxidized to the corresponding *P*-diemthylamino-6-phosphaverdazyl (**5**) as a persistent radical. Analysis of the electron paramagnetic resonance spectrum of **5** revealed significant spin density on the exocyclic nitrogen but very little spin density on the phosphorus, in contrast to the previously reported *P*-phenyl-6-phosphaverdazyl (**4**). Density functional theory calculations on simplified models of **4**, **5**, and related radicals were performed and revealed that spin polarization effects and the nature of the substituents on phosphorus have significant effects on the structures and spin distributions of these radicals. The spin transfer to the dimethylamino group in **5** was revealed to arise from spiroconjugation-type overlap between the nitrogen 2p orbital with the verdazyl radical singly occupied molecular orbital.

## Introduction

Stable radicals contradict the dogma that molecules with open-shell configurations are highly reactive, transient entities. In addition to the sheer novelty of such species, stable radicals have found a wide range of uses, including as spin labels for biomolecules,[3] reagents for polymer synthesis,[4−7] and as constituents of solid-state materials with desirable conducting[8,9] or magnetic[10−14] properties. Most of these "applications" make use of a relatively narrow selection of stable radicals, predominantly based on the nitroxide family.[15] Verdazyls (**1**, **2**) are another known family of stable radicals[16,17] that, despite their robust nature, have not yet attracted much interest in the contexts outlined above. Virtually all the verdazyl literature to date has dealt solely with synthesis and electron paramagnetic resonance (EPR) characterization, although there has been some recent interest in the solid-state magnetic properties of these radicals.[18−23]

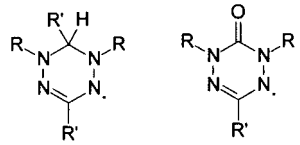

**1** **2**

As part of a program aimed at preparing and studying the properties of new stable radicals, we are exploring the effects of skeletal atom substitution on the electronic structure of the verdazyl ring. To this end, we recently described the syntheses and EPR spectra of verdazyl radicals **3** and **4** containing a single phosphorus atom in various positions of the verdazyl skeleton.[24] Although the gradual decomposition of these radicals precluded growth of single crystals suitable for X-ray diffraction, the EPR spectra (in particular the phosphorus hyperfine coupling constants) of **3** and **4** suggested qualitative differences in their spin distributions and, by inference, their structures. Briefly, the 3-phosphaverdazyl radical **3** has minimal spin density on the phosphorus and is inferred to have a planar ring by analogy to derivatives of the known 6-oxoverdazyls **2**. In contrast, there is

(1) University of Victoria.
(2) Chalmers Tekniska Högskola.
(3) Berliner, L. J. *Spin Labelling: Theory and Applications*; Academic Press: New York, 1979; Vol. 2.
(4) Hawker, C. J. *Acc. Chem. Res.* **1997**, *30*, 373.
(5) Georges, M. K.; Veregin, R. P. N.; Kazmeier, P. M.; Hamer, G. K. *Macromolecules* **1993**, *26*, 2987.
(6) Fischer, H. *Macromolecules* **1997**, *30*, 5666.
(7) Greszta, D.; Mardare, D.; Matyjaszewski, K. *Macromolecules* **1994**, *27*, 638.
(8) Oakley, R. T. *Can. J. Chem.* **1993**, *71*, 1775.
(9) Chi, X.; Itkis, M. E.; Patrick, B. O.; Barclay, T. M.; Reed, R. W.; Oakley, R. T.; Cordes, A. W.; Haddon, R. C. *J. Am. Chem. Soc.* **1999**, *121*, 10395.
(10) Turnbull, M. M.; Sugimoto, T.; Thompson, L. K. *Molecule-Based Magnetic Materials: Theory, Techniques, and Applications*; American Chemical Society: Washington, DC, 1996.
(11) Allinson, G.; Bushby, R. J.; Paillaud, J. L. *J. Mater. Sci.* **1994**, *5*, 67.
(12) Miller, J. S.; Epstein, A. J. *Angew. Chem., Int. Ed. Engl.* **1994**, *33*, 385.
(13) Nakatsuji, S.; Anzai, H. *J. Mater. Chem.* **1997**, *7*, 2161.
(14) Enoki, T.; Yamamura, J. I.; Miyazaki, A. *Bull. Chem. Soc. Jpn.* **1997**, *70*, 2005.
(15) Forrester, A. R.; Hay, J. M.; Thomson, R. H. *Organic Chemistry of Stable Free Radicals*; Academic Press: London, 1968.
(16) Neugebauer, F. A. *Angew. Chem., Int. Ed. Engl.* **1973**, *12*, 455.
(17) Neugebauer, F. A.; Fischer, H.; Siegel, R. *Chem. Ber.* **1988**, *121*, 815.
(18) Allemand, P. M.; Srdanov, G.; Wudl, F. *J. Am. Chem. Soc.* **1990**, *112*, 9391.
(19) Brook, D. J. R.; Lynch, V.; Conklin, B.; Fox, M. A. *J. Am. Chem. Soc.* **1997**, *119*, 5155.
(20) Kremer, R. K.; Kanellakopulos, B.; Bele, P.; Brunner, H.; Neugebauer, F. A. *Chem. Phys. Lett.* **1994**, *230*, 255.
(21) Mukai, K.; Nedachi, K.; Jamali, J. B.; Achiwa, N. *Chem. Phys. Lett.* **1993**, *214*, 559.
(22) Mukai, K.; Kawasaki, S.; Jamali, J. B.; Achiwa, N. *Chem. Phys. Lett.* **1995**, *241*, 618.
(23) Mukai, K.; Nuwa, M.; Suzuki, K.; Nagaoka, S.; Achiwa, N.; Jamali, J. B. *J. Phys. Chem. B* **1998**, *102*, 782.
(24) Hicks, R. G.; Hooper, R. *Inorg. Chem.* **1999**, *38*, 284.

10.1021/ic000939l CCC: $20.00 
Published on Web 03/09/2001

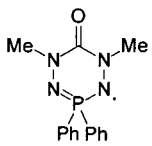

**3**

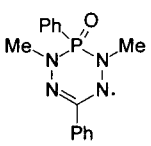

**4**

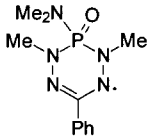

**5**

a significant coupling to the phosphorus atom of 6-phosphaverdazyl **4**, which suggests a nonplanar half-boat conformation by analogy with verdazyls of general structure **1**. In this paper we present the synthesis and characterization of a *P*-dimethylamino-substituted 6-phosphaverdazyl **5**, whose EPR spectrum suggests an electronic and geometric structure different from that of the *P*-phenyl derivative **4**. To gain deeper insights into these radicals, we also present detailed theoretical investigations of the molecular structures and spin distributions of several phosphaverdazyl radicals using density functional theory (DFT) methods.

## Experimental Section

**General.** All reactions and manipulations were carried out under an argon atmosphere using standard Schlenk or glovebox techniques. Solvents were dried and distilled under argon prior to use ($CH_2Cl_2$ and toluene, over $CaH_2$; benzene and THF, over Na/benzophenone). All reagents were purchased from Aldrich and used as received. NMR spectra were recorded on a Bruker AMX360 spectrometer. EPR spectra were recorded on a Bruker EMX300 instrument, and the spectra so obtained were simulated using the SIMFONIA simulation program (Bruker), employing a line width of 1.6 G and a Lorentzian/Gaussian ratio of 0.3. Elemental analyses were carried out by Canadian Microanalytical Services Ltd., Vancouver, B.C.

**Synthesis of *N,N*-Dimethylaminophosphonic Acid Bis(1-methylhydrazide) (6).** A solution of $Me_2NP(O)Cl_2$[25] (9.010 g, 55.6 mmol) in 25 mL of $CH_2Cl_2$ was added dropwise to a solution of methylhydrazine (12 mL, 226 mmol) in 40 mL of $CH_2Cl_2$ at −42 °C (dry ice/acetonitrile bath) under argon. The reaction mixture was stirred for 16 h, and then the white precipitate of methylhydrazine hydrochloride was filtered. The filtrate was evaporated in vacuo to give the product as a hygroscopic oil, yield 80%. The oil was used without further purification. $^1$H NMR ($CD_2Cl_2$): $\delta$ 4.35 (br s, 4H), 2.88 (d, 6H, $^3J_{HP}$ = 8.1 Hz), 2.67 ppm (d, 6H, $^3J_{HP}$ = 9.6 Hz). $^{31}$P NMR ($CDCl_3$): $\delta$ 25.33 ppm. IR ($CH_2Cl_2$): (NH) 3338 (m), 3254 (m), 3170 (m), 1608 (m), 1460 (m), 1300 (s), (P═O) 1194 (s), 995 (s) cm$^{-1}$.

**1,2,5,6-Tetrahydro-1,5-dimethyl-6-(*N,N*-dimethylamino)-6-phenyl-1,2,4,5,6-tetrazaphosphorine-6-oxide (7).** A solution of **6** (4.128 g, 22.8 mmol), trimethyl orthobenzoate (4.0 mL, 23.3 mmol), and acetic acid (10 drops) was refluxed for 16 h in 80 mL of $CH_2Cl_2$. The solvent was then removed and the residue chromatographed on silica gel (1:1 $CH_3CN/CH_2Cl_2$) to give the product as a pink oil that solidified on standing. The solid residue was recrystallized from $CH_3CN$ to give the product as clear prisms, yield 2.56 g (42%). $^1$H NMR ($CD_2Cl_2$): $\delta$ 7.7−7.6 (m, 2H), 7.4−7.3 (m, 3H), 7.01 (d, 1H, N*H*, $^3J_{HP}$ = 8.8 Hz), 3.15 (d, 3H, N−C*H*$_3$, $^3J_{HP}$ = 5.9 Hz), 2.74 (d, 3H, N−C*H*$_3$, $^3J_{HP}$ = 9.6 Hz), 2.64 ppm (d, 6H,N(C*H*$_3$)$_2$, $^3J_{HP}$ = 9.6 Hz). $^{13}$C NMR ($CD_2Cl_2$): $\delta$ 141.4 (d, $J_{CP}$ = 9.0 Hz), 132.8, 130.0, 128.8, 126.7, 39.2 (d, $J_{CP}$ = 5.7 Hz), 37.0 (d, $J_{CP}$ = 4.5 Hz), 36.6 ppm (d, $J_{CP}$ = 7.9 Hz). $^{31}$P NMR ($CD_2Cl_2$): $\delta$ 7.11 ppm. IR (KBr): $\nu$(NH) 3187 (s), 1606 (s), 1570 (m), 1515 (s), 1489 (s), 1462 (s), 1445 (s), 1325 (m), 1304 (s), 1255 (s), 1224 (s), 1200 (s) 1185 (s), 1144 (s), 1124 (s), 1083 (m), 1068 (m), 1029 (w), 995 (s), 959 (s), 931 (s), 773 (s), 764 (s), 749 (s), 691 (s), 633 (w), 621 (w), 595 (w), 523 (s), 497 (m), 467 (m), 406 (m) cm$^{-1}$. UV, $\lambda_{max}$ ($CH_2Cl_2$): 296, 231 nm. Mp: 151−153 °C. Anal. Calcd for $C_{11}H_{18}N_5OP$: C, 49.43; H, 6.79; N, 26.20; P, 11.59. Found: C, 49.45; H, 6.62; N, 25.92; P, 10.93. MS (CI methane): *m*/*z* 268 (M + 1, 100%), 296 (M + 29, 12%).

(25) Walsh, E. N.; Toy, A. D. F. *Inorg. Synth.* **1963**, *7*, 69.

Scheme 1[a]

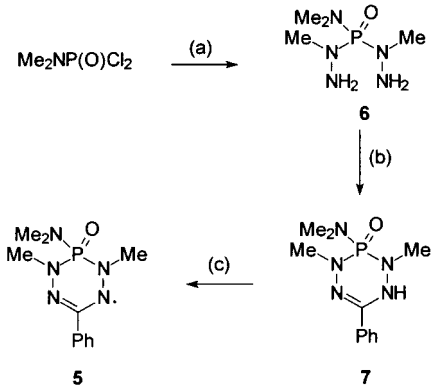

[a] Reagents: (a) $MeNHNH_2$ (4.5 equiv); (b) $PhC(OMe)_3$; (c) benzoquinone.

**1,5-Dimethyl-6-(*N,N*-dimethylamino)-6-oxo-3-phenyl-6-phosphaverdazyl (5).** Benzoquinone (23 mg, 0.213 mmol) was added to a solution of **7** (102 mg, 0.382 mmol) in 10 mL of benzene. The solution immediately turned intense red. The solution was stirred for 30 min, and then the solvent was removed under reduced pressure to leave a red semisolid. The residue was chromatographed (alumina, activity II−III, $CH_2Cl_2$) to afford **5** as a red oil. UV, $\lambda_{max}$ ($CH_2Cl_2$): 295, 229, 538 nm. Solutions of this radical decomposed within a day or two, and solid material also decomposed over several days, predominantly to the tetraazaphosphorine **7**. Freshly prepared solutions of **5** could be quantitatively (as monitored by $^1$H NMR) reduced back to **7** using ascorbic acid as a reducing agent.

**Computational Details** All calculations were made with the DFT module in Spartan 5.1.3a1.[26] Geometries were fully optimized without symmetry constraints, employing the exchange and correlation functionals of Becke[27] and Perdew,[28,29] respectively (BP86), together with an extra fine integration grid. A numerical basis set, DN*, including polarization and d functions for C, N, O, and P, was used. This basis set is roughly equivalent in "size" to the 6-31G* basis set but is claimed to yield results closer to much larger Gaussian basis sets.[30] In no case was the spin contamination larger than 1%.

## Results

**Synthesis and EPR Spectrum of 5.** Radical **5** was prepared by extension of the methodology used to synthesize **4** as shown in Scheme 1. The *P*-(dimethylamino)-substituted bis(hydrazide) **6** was prepared by reaction of the corresponding phosphonic acid dichloride with an excess of methylhydrazine. Subsequent reaction of **6** with trimethyl orthobenzoate afforded the tetraazaphosphorine **7**. The asymmetry of the ring in **7** renders the protons of the two ring-substituted *N*-methyl groups distinct in terms of their $^1$H chemical shifts ($\delta$ = 3.15 vs 2.74 ppm) and their coupling constants to the phosphorus nucleus ($J_{PH}$ = 5.9 vs 9.6 Hz). Oxidation of **7** with benzoquinone afforded **5** as a persistent radical that slowly decomposed in solution or the solid state. The solution EPR spectrum of **5** and the corresponding simulated spectrum is shown in Figure 1. Spectral simulation afforded the hyperfine coupling constants contained in Table 1, along with EPR parameters for some related (phospha)verdazyl radicals. For **5** the hyperfine coupling constants to the four nitrogen atoms of the verdazyl ring and the six *N*-methyl protons are consistent with related verdazyls.

(26) *SPARTAN 5.1.3A1*; Wavefunction, Inc.: Irvine, CA, 1998.
(27) Becke, A. D. *Phys. Rev. A* **1988**, *38*, 3098.
(28) Perdew, J. P. *Phys. Rev. B* **1986**, *33*, 8822.
(29) Perdew, J. P. *Phys. Rev. B* **1986**, *34*, 7406.
(30) Hehre, W. J.; Yu., J.; Klunzinger, P. E. *A Guide to Molecular Mechanics and Molecular Orbital Calculations in Spartan*; Wavefunction, Inc.: Irvine, CA.

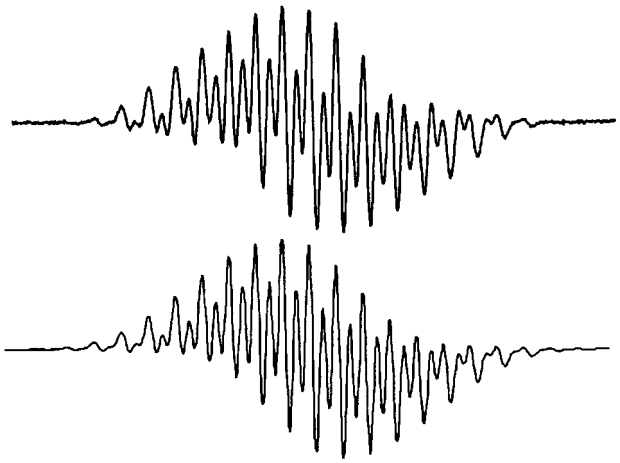

**Figure 1.** Experimental (top) and simulated (bottom) EPR spectrum of **5** in $CH_2Cl_2$. Sweep width is 100 G.

In addition, the simulated spectrum includes substantial coupling to the *exocyclic* nitrogen atom as well as the six protons of the methyl groups attached to it, but *not* the phosphorus atom. The observation of coupling to the former nitrogen is not unexpected, although the magnitude of the constant is perhaps surprising. More unusual is the lack of coupling to the phosphorus, which strongly contrasts with radical **4**, which has a relatively large *a*(P) of 5.2 G. We note that the simulated spectrum contains low-intensity peaks (not shown) on the outer wings of the spectrum that are not observable in the experimental spectrum because of baseline noise in the latter. The inability to see these experimental peaks, in combination with the complexity of the spectrum, renders the assignment of hyperfine coupling constants somewhat tentative; as such, we cannot conclusively rule out the possibility that a completely different set of constants that includes a nonzero *a*(P) value exists.

**Computational Studies.** The three phosphorus-containing verdazyls **3**−**5** present a rich array of EPR spectra and structural possibilities. The lack of long-term stability has unfortunately prevented us from obtaining experimental structural information on these new radical species. To gain a better understanding of the effects of both skeletal and substituent substitution on the electronic structures of phosphaverdazyl radicals, we therefore performed calculations on structures **2a**−**5a**, which are simplified models for radicals **2**−**5**, respectively. In particular we wanted to assess the spin distributions in these compounds and how they are related to the presence and position of the phosphorus atom in the ring, as well as substituent effects.[31] DFT methods have recently been employed to understand the magnetic properties and mechanisms of spin polarization in verdazyl radicals.[32,33] In general, DFT methods have been shown to give good agreement with spin densities derived from polarized neutron diffraction[34−37] and NMR[33,38] experiments and also to give good estimates of magnetic interactions[39] and EPR hyperfine coupling constants.[40−44]

**Table 1.** EPR Parameters for Selected (Phospha)verdazyl Radicals[a]

| | **2** (R = Me, R′ = Ph)[b] | **3**[c] | **4**[c] | **5**[d] |
|---|---|---|---|---|
| *g* | 2.0037 | 2.0038 | 2.0038 | 2.0037 |
| $a(N_{2,4})$ | 6.5 | 6.4 | 6.4 | 6.5 |
| $a(N_{1,5})$ | 5.3 | 5.3 | 4.4 | 4.3 |
| $a(CH_3)$ | 5.3 | 5.4 | 4.6 | 4.6 |
| *a*(P) | | 0.2 | 5.2 | 0 |
| *a*(N′) | | | | 4.6 |
| $a(CH_3')$ | | | | 4.5 |

[a] Hyperfine coupling constants are in G. $N_{2,4}$ refers to the two-coordinate nitrogens, $N_{1,5}$ to the three coordinate nitrogen, and N′ to the exocyclic nitrogen in **5**. [b] Reference 17. [c] Reference 24. [d] This work.

**Table 2.** DFT Spin Population Analyses for the Optimized Structures of **2a**−**4a**

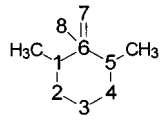


| | **2a** | **3a** | **4a** | **4a′** | **4a″** |
|---|---|---|---|---|---|
| $N_{1,5}$ | 0.205 | 0.221 | 0.178 | 0.182 | 0.180 |
| $N_{2,4}$ | 0.341 | 0.290 | 0.327 | 0.306 | 0.328 |
| 3 | (C) −0.087 | (P) −0.002 | (C) −0.089 | −0.074 | −0.079 |
| 6 | (C) −0.020 | (C) −0.036 | (P) 0.013 | 0.027 | 0.031 |
| $O_7$ | −0.013 | −0.025 | −0.004 | −0.006 | −0.003 |
| 8 | | | (C) −0.009 | −0.009 | 0.000 |
| 1,5-$CH_3$ | 0.009 | 0.011 | 0.009 | 0.009 | 0.009 |

The total Mulliken spin populations are given in Table 2 for **2a**, **3a** (for which one stationary point each was obtained), and the three stationary points found for **4a**.[45] We begin our discussion of structure/property correlations in verdazyl radicals with some experimental observations for the "parent" systems **1** and **2.** Crystallographically characterized derivatives of these radicals indicate that the verdazyl ring may be either planar or bent depending on the nature of the C6 carbon atom. So-called "6-oxoverdazyls" **2** bearing a carbonyl group are planar[46,47] presumably because of the amide-type resonance interaction between the lone pairs on the flanking nitrogens (N1 and N5) and the carbonyl $\pi^*$ orbital. Verdazyls of general structure **1** lack such conjugative possibilities, and consequently, the

(31) We have not attempted to calculate the actual values of the hyperfine coupling constants because this requires more care in the choice of method, basis functions, and the calculation of Fermi contact terms. The contribution of several conformers also complicates the case. Note that the spin densities alone cannot be expected to correlate quantitatively with the hyperfine coupling constants. We do note, however, a general trend of higher spin population with higher reduced coupling constant (*J*/magnetogyric moment).

(32) Green, M. T.; McCormick, T. A. *Inorg. Chem.* **1999**, *38*, 3061.
(33) Ohrstrom, L.; Grand, A.; Pilawa, B. *Acta Chem. Scand.* **1996**, *50*, 458.
(34) Romero, F. M.; Ziessel, R.; Bonnet, M.; Pontillon, Y.; Ressouche, E.; Schweizer, J.; Delley, B.; Grand, A.; Paulsen, C. *J. Am. Chem. Soc.* **2000**, *122*, 1298.
(35) Pontillon, Y.; Caneschi, A.; Gatteschi, D.; Grand, A.; Ressouche, E.; Sessoli, R.; Schweizer, J. *Chem.—Eur. J.* **1999**, *5*, 3616.
(36) Gillon, B.; Aebersold, M. A.; Kahn, O.; Pardi, L.; Delley, B. *Chem. Phys.* **1999**, *250*, 23.
(37) Pontillon, Y.; Akita, T.; Grand, A.; Kobayashi, K.; Lelievre-Berna, E.; Pecaut, J.; Ressouche, E.; Schweizer, J. *J. Am. Chem. Soc.* **1999**, *121*, 10126.
(38) Maruta, G.; Takeda, S.; Yamaguchi, A.; Okuno, T.; Awaga, K.; Yamaguchi, K. *Mol. Cryst. Liq. Cryst.* **1999**, *334*, 296.
(39) Reznikov, V. A.; Ovcharenko, I. V.; Pervukhina, N. V.; Ikorskii, V. N.; Grand, A.; Ovcharenko, V. I. *Chem. Commun.* **1999**, 539.
(40) Raiti, M. J.; Sevilla, M. D. *J. Phys. Chem. A* **1999**, *103*, 1619.
(41) Braden, D. A.; Tyler, D. R. *Organometallics* **1998**, *17*, 4060.
(42) O'Malley, P. J. *J. Phys. Chem. A* **1997**, *101*, 9813.
(43) Niemz, A.; Rotello, V. M. *J. Am. Chem. Soc.* **1997**, *119*, 6833.
(44) Adamo, C.; Matteo, A. d.; Rey, P.; Barone, V. *J. Phys. Chem. A* **1999**, *103*, 3481.
(45) The replacement of the phenyl group in position 3 by hydrogen causes only small differences in geometry and spin densities. Calculations on a model compound **2b** in which R = $CH_3$ and R′ = Ph show the main effect to be a 17% overestimation of the spin polarization on the carbon in position 3; there is no contribution of the phenyl group to the SOMO orbital. However, the net spin density on C3 in **2a** equals the sum of spin densities on C3 and the phenyl group in **2b**.
(46) Brook, D. J. R.; Fox, H. H.; Lynch, V.; Fox, M. A. *J. Phys. Chem.* **1996**, *100*, 2066.
(47) Neugebauer, F. A.; Fischer, H.; Krieger, C. *J. Chem. Soc., Perkin Trans. 2* **1993**, 535.

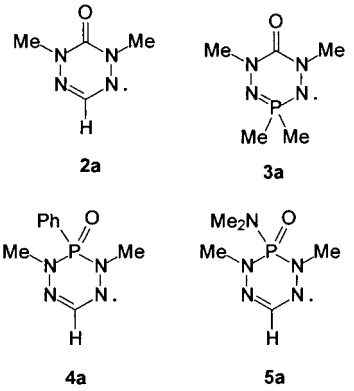


methylene group is raised above the plane of the ring, producing a half-boat conformation.[48]

Radical **2a** is the prototypical member of the 6-oxoverdazyl family **2**, whereas **3a** is a simpler version of 3-phosphaverdazyl **3**, which we recently reported.[24] The DFT-optimized structures of **2a** and **3a** are both essentially planar (see Supporting Information), but there are subtle differences in the electronic structures of the two radicals. The singly occupied molecular orbitals (SOMO) and next highest (doubly occupied) orbital (NHOMO) of **2a** and **3a** are presented in Figure 2. The SOMOs of these two radicals are practically the same; the four ring nitrogens account for about 90% of the spin density. Spin polarization of the NHOMOs leads to large negative spin densities on atoms that have a node in the SOMO *and* have a large component in the NHOMO (cf. allyl radical). The SOMO in **2a** has nodes at O1, C6, and C3, but for C6 there is also a node in the next highest occupied $\pi$ orbital (NHOMO). Thus, C3 is predicted to possess negative spin density ($-0.087$) while the carbonyl group (C6) has a lower spin density ($-0.020$).

In **3a** a curious situation arises at the phosphorus atom. Details of the population analysis reveal a significant ($\sim$3%) P($d_{xz}$) contribution to the SOMO. This positive spin density is essentially countered by negative spin density arising from polarization of the PN $\sigma$ bonds, resulting in a negligible total spin population ($-0.003$) at the phosphorus. This corroborates our experimental studies on 3-phosphaverdazyl **3**: simulation of the EPR spectrum of this radical produced a hyperfine coupling constant to P of 0.2 G as an upper limit.

The structure and spin populations for the 6-phosphavderazyl radicals **4a** and **5a** contrast with those for 3-phosphaverdazyl **3a**. Three conformers of **4a** (referred to as **4a**, **4a′**, and **4a″**) were obtained as stationary points and are shown in Figure 3. The six-membered ring of conformer **4a** is essentially flat—the N1−P6−N5 moiety forms a dihedral angle of 6° with the plane of the ring defined by atoms 1−5 (i.e., all but the P)—whereas in **4a′** and **4a″** the phosphorus is bent out of the plane, producing half-boat conformations with dihedral angles of 30° and 38°, respectively. The P-phenyl ring is oriented nearly parallel to the P═O bond in **4a** and **4a′**, whereas in **4a″** the phenyl group is rotated by 90° with respect to this bond. The relative energies of the three structures are quite similar (**4a**, 0; **4a′**, +1.2; **4a″**, +3.2 kcal mol$^{-1}$), which seems to indicate that this 6-phosphaverdazyl does not have a strong preference for a bent vs planar structure. The P═O bond might be expected to act as a $\pi$ acceptor analogously to the carbonyl group in the 6-oxoverdazyls, which would favor the planar ring conformation **4a**. However, the tetrahedral nature of four-coordinate phosphorus forces the P═O bond out of the plane of the ring, thereby precluding any such overlap.

(48) Williams, D. E. *Acta Crystallogr.* **1973**, *B29*, 96.

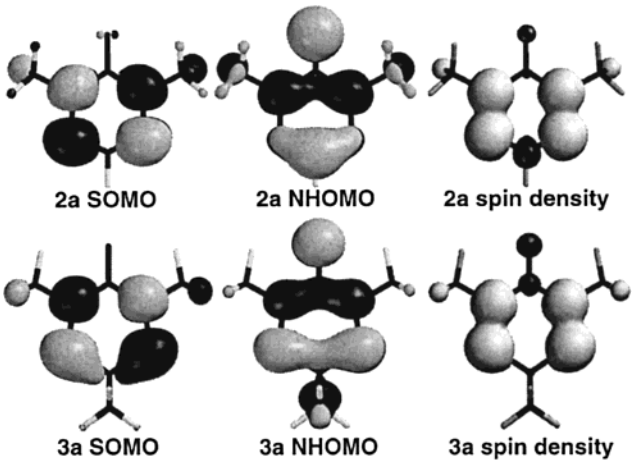


**Figure 2.** Singly occupied molecular orbitals (SOMO), next-highest (doubly) occupied orbitals (NHOMO), and spin density plots for radicals **2a** and **3a**.

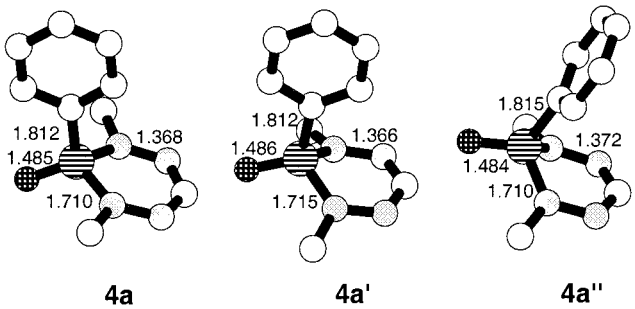


**Figure 3.** DFT optimized structures and relative energies of **4a**, **4a′**, and **4a″** with selected bond lengths. Hydrogen atoms have been omitted for clarity.

The phosphorus spin populations are larger for the bent geometries, 0.027 and 0.030 for **4a′** and **4a″** versus 0.013 for **4a**. In all three of the models of **4** the SOMO mixing with phosphorus d orbitals are more or less constant. However, in the optimized bent geometries the P═O bond is almost (18° for **4a″**) parallel to the verdazyl plane, only slightly removed from it by the bend of the N−P−N unit. This results in a small interaction between the P═O $\pi$ bond and the verdazyl $\pi$ system via the P($p_x$) and O($p_x$) orbitals. There is thus direct mixing of phosphorus atomic orbitals into the SOMO, and the net spin is positive for the bent conformers, whereas the mixing of p orbitals completely disappear in the planar geometry. Moreover, both **4a** and **4a′** show sizable spiro interactions in the SOMO, resulting in spin populations of 0.02 at the ortho and para carbon atoms, although the spin population at the ipso carbons is much smaller.

Three stationary points were also found for the dimethylamino-substituted phosphaverdazyl (**5a**, **5a′**, and **5a″**) (see Supporting Information). Conformer **5a**, the lowest energy structure, is only slightly bent, with the NPN moiety bent out of the ring plane by 17°. The other two structures **5a′** (2.4 kcal higher in energy than **5a**) and **5a″** (19.4 kcal higher) are significantly more bent, with corresponding dihedral angles of 35° and 50°, respectively. The dimethylamino nitrogen atom is nearly planar in **5a** (sum of the angles is 357°), and the CNC plane of this group forms a dihedral angle of 20° with the P═O bond. The ideal perfectly symmetric ($C_s$) version of structure **5a** (for which the latter dihedral would be 0°) was found to be the transition state for the observed stationary point **5a**, and the calculated inversion barrier was very low (+0.2 kcal/mol). In structure **5a′** the $Me_2N$ nitrogen is slightly

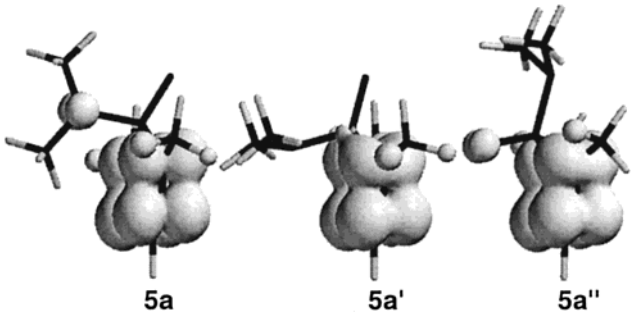


**Figure 4.** Plot of the positive (α) spin densities of **5a, 5a′**, and **5a′′** (boundary 0.002).

**Table 3.** DFT Spin Population Analyses for the Three Optimized Geometries of **5a**[a]

| | **5a** | **5a′** | **5a′′** |
|---|---|---|---|
| $N_{1,5}$ | 0.179, 0.201 | 0.179, 0.185 | 0.201 |
| $N_{2,4}$ | 0.320 | 0.331 | 0.316 |
| $C_3$ | −0.087 | −0.081 | −0.078 |
| $P_6$ | −0.014 | −0.024 | 0.015 |
| $O_7$ | −0.001 | −0.005 | 0.034 |
| $N_8$ | 0.044 | −0.003 | −0.001 |
| 1,5-C$H_3$ | 0.009 | 0.01 | 0.007 |

[a] See Table 2 for atom position definitions.

pyramidal (sum of angles is 350°) and the group is rotated by about 90° with respect to the orientation in **5a**. The dimethylamino group in **5a′′** occupies the pseudoequatorial position (as opposed to the axial position for **5a** and **5a′**), and the nitrogen is much closer to a "normal" pyramidal geometry (sum of angles is 333°). Further comparisons between **5a** and **5a′** are noteworthy: The dimethylamino groups are related to one another in these structures by rotation about the exocyclic P−N bond. The activation barrier for this process was calculated to be 6 ± 2 kcal/mol and may arise because of the loss of overlap between the nitrogen 2p orbital with the verdazyl $\pi$ system (see later). The relatively low barrier to rotation, in combination with the small energy differences between **5a** and **5a′**, leads us to conclude that the observed EPR hyperfine coupling for **5** probably represents a weighted average of conformations **5a** and **5a′**.

Spin density plots for the three structures (Figure 4) shed light onto the means by which spin density "leaks" onto the exocyclic nitrogen; spin density populations for each structure are presented in Table 3. The spin density in **5a** clearly contains a substantial contribution from the exocyclic nitrogen p orbital. The spin population on this atom is much higher than on the corresponding ipso carbon atom in any of the structures of P-phenyl derivative **4a**. In structure **5a′** the orientation of the nitrogen p orbital is incorrect for overlap with the verdazyl $\pi$ SOMO (an antibonding MO that possesses a nodal plane running along the molecule's pseudomirror plane), and as a result, this isomer yields essentially no spin density on the nitrogen. In **5a′′** the dimethylamino group is remote from the verdazyl ring, and so there is no spin density there. Spiroconjugation does produce some spin on the P═O oxygen for this structure, but experimentally this cannot be detected by EPR at $^{13}C$ natural abundance levels.

## Discussion

Knowledge of the structure and spin distributions in new stable radicals is crucial if the chemical or physical properties of these radicals are to be exploited. The lack of structural information on phosphorus-containing verdazyls, coupled with the diversity in structures and spin distributions suggested by our EPR data, necessitated the DFT calculations that have been presented herein. Our DFT calculations, in combination with the aforementioned EPR data, have provided a clearer picture of the perturbation that phosphorus atom substitution has on verdazyl radicals. There is a qualitative agreement between the EPR spectra and the DFT-calculated spin populations in compounds **2**−**5**, although a number of competing factors preclude definitive agreements. In general we have found that the composition of the SOMOs of the various (phospha)verdazyl radicals is qualitatively similar, differing mainly by the small contributions of the phosphorus in the 6-position. However, spin polarization effects are critical and appear to have strong implications for the structures and in particular the spin distributions in these radicals. The most striking example of this is the apparent changes in structure and spin distribution between 6-phosphaverdazyl radicals **4** and **5**, which differ only by the substituent on the phosphorus. In chemical terms, the exocyclic dimethylamino group of **5** acts as a $\pi$ donor with respect to the phosphorus and/or the verdazyl ring. This is borne out by the structural features of optimized model **5a**: the $Me_2N$ is nearly planar at the nitrogen, the PN bond is shortened compared to the other two isomers, and the ring appears to favor a nearly planar structure; in P-phenyl derivative **4a** the strength of this interaction is diminished. The specific reasons behind these effects are not clear, and the balance of a number of effects on the actual structures and spin distributions is clearly a subtle one. We do note that in many *diamagnetic* PN ring systems (i.e., cyclophosphazenes, $(R_2PN)_n$), ring conformations are very sensitive to the nature of the substituents on the phosphorus.[49]

Perhaps the most intriguing development is the theoretical and experimental observation of substantial spin density on an exocyclic group in radical **5**. DFT calculations confirm that this arises from a through-space interaction between the verdazyl SOMO and the nitrogen p orbital in a manner that can be accurately described as spiroconjugation.[50,51] This is depicted schematically in **8** as viewed down the end of the molecule.

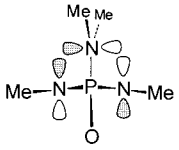


**8**

Spiroconjugation in radicals has been a considerable topic for discussion in recent years[9,52−58] and may offer a new mechanism for spin propagation or spin coupling that fundamentally differs from the more conventional spin delocalization/polarization mechanisms involving $\pi$ conjugation. In **5**, the experimental

(49) Allcock, H. R. *Chem. Rev.* **1972**, *72*, 315.
(50) Simmons, H. E.; Fukunaga, T. *J. Am. Chem. Soc.* **1967**, *89*, 5208.
(51) Durr, H.; Gleiter, R. *Angew. Chem., Int. Ed. Engl.* **1978**, *17*, 559.
(52) Hoffmann, R.; Imamura, A.; Zeiss, G. D. *J. Am. Chem. Soc.* **1967**, *89*, 5215.
(53) McElwee-White, L.; Goddard, W. A., III; Dougherty, D. A. *J. Am. Chem. Soc.* **1984**, *106*, 3461.
(54) McElwee-White, L.; Dougherty, D. A. *J. Am. Chem. Soc.* **1984**, *106*, 3466.
(55) Haddon, R. C.; Mayo, S. L.; Chichester, S. V.; Marshall, J. H. *J. Am. Chem. Soc.* **1985**, *107*, 7585.
(56) Haddon, R. C.; Chichseter, S. V.; Marshall, J. H. *Tetrahedron* **1986**, *42*, 6293.
(57) Haddon, R. C.; Chichester, S. V.; Mayo, S. L. *Inorg. Chem.* **1988**, *27*, 1911.
(58) Frank, N. L.; Clerac, R.; Sutter, J. P.; Daro, N.; Kahn, O.; Coulon, C.; Green, M. T.; Golhen, S.; Ouahab, L. *J. Am. Chem. Soc.* **2000**, *122*, 2053.

manifestation of spiroconjugation is the observation of a significant EPR hyperfine coupling to the exocyclic nitrogen. There may also be some spin density on the carbons of the P-phenyl group in **4** through an analogous mechanism, but the low natural abundance of $^{13}C$ precludes its detection by EPR. As noted earlier, the hyperfine coupling in **5** to the $Me_2N$ group probably represents a weighted sum of contributions of various conformers because of the relative ease of PN bond rotation and $Me_2N$ inversion. This suggests that 6-phosphaverdazyl derivatives with conformationally rigid $\pi$ donor groups may exhibit spin propagation that is even more pronounced than in the present compounds.

**Acknowledgment.** R.G.H. thanks the Natural Sciences and Engineering Research Council of Canada and the University of Victoria for Financial Support. L.Ö. thanks the Swedish Research Council for Engineering Sciences and Stiftelsen för Strategisk Forskning for financial support.

**Supporting Information Available:** Optimized structures of **2a, 3a**, **5a**, **5a′**, and **5a″** and coordinate files for all optimized structures (.pdb format, suitable for Spartan/ChemDraw). This material is available free of charge via the Internet at http://pubs.acs.org.

IC000939L